Integrated infection and crowd behavior model for COVID-19 infection risk assessment onboard large passenger vessels

de Haan, N.A.; Kana, A.A.; Atasoy, B.

DOI
10.59490/imdc.2024.867

Publication date
2024

Document Version
Final published version

Published in
Proceedings of the 15th International Marine Design Conference (IMDC-2024)

Proceedings of 15th International Marine Design Conference (IMDC-2024)
June 2-6, 2024
Amsterdam, the Netherlands

Integrated infection and crowd behavior model for COVID-19 infection risk assessment onboard large passenger vessels

N.A. de Haan[1], A.A. Kana[1,2,*] and B. Atasoy[1,3]

ABSTRACT

The development of the global COVID-19 pandemic from 2020 onward has had significant impact on the world and specifically the maritime industry. Striking examples were COVID-19 outbreaks onboard the Diamond Princess cruise vessel and the U.S.S. Theodore Roosevelt aircraft carrier at the start of the pandemic. Contagious disease management onboard large passenger ships remains a complex issue, amplified by the international character of the industry, confined environment and shared facilities. This paper therefore presents an integrated infection and crowd behavior model used to calculate agent-specific infection risk, incorporating guest and crew circulation through a passenger ship layout. The integrated model is used to investigate the effect of ship layout design, capacity reduction and mask wearing on COVID-19 airborne infection risk onboard large passenger vessels.

KEY WORDS

Contagious disease; passenger vessel; layout design; COVID-19; infection risk

INTRODUCTION

The development of the global COVID-19 pandemic from 2020 onward has had a significant impact on the world and specifically the maritime industry. The shipping industry had to deal with restricted travel, changing trade volumes, increased waiting times and stricter security measures in ports (Yazir et al., 2020). As seafarers kept working through the COVID-19 pandemic, quarantines, travel restrictions and country entering measures became standard practice (Keçeci, 2022). Striking examples of the pandemic's impact were COVID-19 outbreaks onboard the Diamond Princess cruise vessel and the U.S.S. Theodore Roosevelt aircraft carrier at the start of the pandemic. During these outbreaks, over 20% of the total population tested positive for SARS-CoV-2 with major implications (Kasper et al., 2020; Turvold and Mcmullin, 2020). Contagious disease management onboard large passenger ships remains a complex issue, amplified by the international character of the industry, confined environment and shared facilities. This paper therefore aims to:

Investigate the effect of ship layout design, capacity reduction and mask wearing on COVID-19 airborne infection risk onboard large passenger vessels

Since the COVID-19 pandemic, significant research has been done into the characteristics of this contagious coronavirus, covering incubation periods, (asymptotic) infection rates and transmission mechanisms (Zhao et al., 2022; Rocklöv et al.,

[1] Department of Maritime and Transport Technology, Delft University of Technology, Delft, the Netherlands
[2] ORCID: 0000-0002-9600-8669
[3] ORCID: 0000-0002-1606-9841
[*] A.A.Kana@tudelft.nl

Submitted: 23 February 2024, Revised: 30 April 2024, Accepted: 1 May 2024, Published: 21 May 2024

Conference paper, DOI: https://doi.org/10.59490/imdc.2024.867 e-ISSN: 3050-4864

2021; Lipsitch et al., 2020). Other literature focuses on ways to prevent or control disease spread, like the research by Gupta et al. (2021) discussing the choice between ship quarantine or disembarkation of suspected cases and the article by Li et al. (2021) proposing "A timeline and system framework for cruise ship disease risk management". Additionally, there is a wide availability in research relating COVID-19 disease spread to behavioral measures like mask wearing, social distancing and personal hygiene. Besides operational and behavioral measures, layout adjustment might be an option for disease prevention and control. This can be connected to the concept of prevention through design (PtD) Brewster et al. (2020). The layout design should thus aim to prevent a disease outbreak and facilitate disease control in case prevention fails. Research connecting ship layout design with contagious disease was done by Ruggiero et al. (2008) as they present a retrofit design for an Italian fast medical support vessel. Furthermore, the Healthy Sailing HORIZON EUROPE research project specifically supports "substantially reducing the spread of communicable disease on board passenger ships" (Healthy Sailing, 2024).

The novelty of this paper lies with the integrated infection and crowd behavior model used to calculate agent-specific airborne infection risk, incorporating guest and crew circulation through a passenger ship layout. These location- and agent-based infection risks can be considered complementary to COVID-19 studies onboard large passenger vessels presenting retrospectively calculated attack rates and reproduction numbers (Rocklöv et al., 2021; Mizumoto and Chowell, 2020; Liu et al., 2020; Rosca et al., 2022).

The scope of this paper is described by the details in the research objective. The ship type is defined and the scope of the measures and interventions tested is limited to capacity reduction, mask wearing and ship layout adaptions. The effect of these measures will be investigated by means of model simulations. The study of ventilation and ventilation system design onboard large passenger vessels in relation to contagious disease spread falls outside the scope of this research.

This paper starts by describing the required background information related to contagious disease transmission, disease prevention and control. This background leads into the development of the integrated model. The first part of the method covers the model requirements where after a specific movement model and infection model were selected for integration. The second part of the method handles the model architecture implemented in order to integrate the movement and infection model. Three interventions are investigated using the integrated model and the results are compared against two sample cases. The interventions feature layout adjustments, capacity reductions and mask wearing. The paper closes with a discussion and concluding summary.

BACKGROUND

Diseases have been a part of daily human life throughout history and the recent COVID-19 pandemic showed the impact of a contagious disease on a global level. Next to coronaviruses; Tuberculosis, Noroviruses and influenza have been linked to life at sea (Mangili and Gendreau, 2005; Kak, 2007). These diseases can spread via four modes of disease transmission as described by Mangili and Gendreau (2005):

- *Contact transmission*
  Contact transmission includes person-to-person contact, contact with a contaminated intermediate host and large droplet transmission; if someone for example inhales large droplets generated when an infector sneezes or coughs. The contaminated intermediate host might be something like a surface or door handle. The densely populated environment, confined and shared spaces onboard large passenger vessels may amplify contact transmission.
- *Airborne transmission*
  Airborne transmission covers very small droplet residua (nuclei) that travel over long distances. These aerolized infectious agents move around because of circulation inside a space, mechanical ventilation or they end up in filtration systems (Tan et al., 2022).
- *Common vehicle transmission*
  Common vehicle transmission route is associated with food and water sources.

- *Vector-borne transmission*
  Vector-borne transmission relies on insects or rodents to spread a disease.

Measures to prevent or control disease transmission onboard large passenger vessels cover three categories: ship layout adjustments, operational measures and behavioral measures. An improved ship layout could feature additional medical facilities, optional isolation and quarantine zones and a lower passenger-space ratio (Rosca et al., 2022; Li et al., 2021). Also, high-risk spaces might benefit from an area or location change. Possibilities for operational measures are: embarkation requirements, extensive onboard disease management and monitoring, and restricted movement onboard or on-shore (Mouchtouri et al., 2010; Kordsmeyer et al., 2021; Moon and Ryu, 2021). Another measure with large potential can be found in the research by Guagliardo et al. (2022). They investigate the effect on COVID-19 infection cases when the general capacity onboard a cruise ship is reduced. The last group of measures is related to the behavior of crew and guests who can improve their personal hygiene, get vaccinated, keep a social distance and wear personal protective equipment like a mask (Noakes et al., 2006; Nicolaides et al., 2020; Kak, 2007; Sun and Zhai, 2020).

METHOD

The development of the integrated movement and infection model followed a two-step approach. The first step is the integrated model analysis. In this step, the model requirements are presented after which a model combination is selected from the various investigated movement and infection models. The second step describes the developed model architecture in order to achieve integration between the movement and infection model.

Integrated Model Requirements

The integrated model requirements are given in Table 1. These requirements can be connected to the scope and specific boundaries of this research. R1 and R9 are related to the considered design stage as converging results are required within a time frame that is acceptable for *initial stage retrofit design*. R2 specifies the population size which is related to the ship type: *large passenger vessels*. The preferred result of this investigation is the *limitation of contagious disease spread* which can be linked to R3 and R12. R10 and R11 specify requirements to monitor the time spent in specific spaces and the space occupation. These requirements can be used to inform *layout adjustments* and the exposure time and space occupation might be relevant when implementing *operational and behavioral measures*. Finally, R4 up to R8 are formulated to achieve two key model specifications: *incorporating crew and guest circulation* and *incorporating movement through a ship layout*.

Keeping the requirements in mind, different types of agent movement and infection models were investigated. Both the investigated movement and infection models describe varying levels of detail, from macroscopic pipe flow models to microscopic agent-based movement models. Widely used compartment models, infection risk models and complex agent-based models were investigated as options to cover the medical aspect of the integrated model. The movement and infection models were brought together in twelve combinations and their integration compatibility was evaluated. After careful consideration, the combination of a mesoscopic route-choice model developed by Narayan et al. (2021) as used in van Gisbergen (2022) and the modified Wells-Riley infection model presented by Sun and Zhai (2020) was selected. Comparing all model combinations against the requirements, this option showed the most potential. The combination is less complex and time-intensive than an agent-based model but it does provide a strong disease performance indication. The performance indication is layout dependent and agent specific.

Table 1: Integrated model requirements

Requirement		Details
1	Convergence	The simulation results converge within an acceptable time frame
2	Population size	3000-4000 Individual agents can be modelled (guests and crew)
3	Disease performance indication	Model results indicate scenario performance for contagious disease spread
		Model results indicate *where* in the layout agents are most at risk for infection
		Model results enable performance comparison between different scenarios
4	Layout incorporation	Model is layout dependent
		Model support layout dimensions from 5 up to 50 meters per space.
5	Space capacity and flow	Model takes limited capacity of spaces into account
		Model takes limited flow between spaces into account
6	Individual movement	Movement can be modelled for each individual agent
		Individual agent movement can be tracked and movement data is stored
7	Random movement	There is controlled randomness in the activities that agents undertake
		There is controlled randomness in *when* agents start different activities
		There is controlled randomness in the routes agents take to their destinations
8	Multi-leg movement	Agents can move between multiple destinations in one simulation
		The time an agent stays at a single destination can be adjusted
9	Medical complexity	Medical model is as simple as possible while producing relevant results
10	Time spent	Time spent at each location is known for every agent
		Time spent at each location is incorporated when calculating infection risk
11	Space occupation	Space occupation is known for each time step
		Space occupation changes with the agents entering and exiting spaces
		Space occupation is incorporated when calculating infection risk
12	Disease specific	Model should (to a degree) take differences between diseases into account

Integrated Model Architecture

The chosen route choice model simulates the normal-day movement of guests and crew onboard a cruise ship based on an activity schedule. The activity schedule provides the destinations and duration of activities while the agents choose their individual routes between destinations based on a mixed logit route choice model. The agents can hold four different states in the route choice model: activity, wayfinding, stay and walk. The ship layout is converted into nodes representing one or multiple spaces and these nodes are connected via bi-directional links.

The implemented infection model presented by Sun and Zhai (2020) calculates Wells-Riley infection probability for airborne disease transmission in confined spaces, taking the social distance into account. The social distance index is shown in Equation 1 where d equals the social distance in meters. The modified Wells-Riley infection risk is given in Equation 2 with the following parameters: P_I: probability of infection, C: new cases, S: susceptible individuals, I: number of infectors, p: pulmonary ventilation rate of susceptible individuals $[m^3/s]$, q: quanta production rate per infected individual [q/s], t: time [s], Q: room ventilation rate $[m^3/s]$ and E_z: ventilation index.

$$P_d = \frac{-18.19\ ln(d) + 43.276}{100} \tag{1}$$

$$P_I = \frac{C}{S} = 1 - exp(-P_d \frac{Iqpt}{QE_z}) \tag{2}$$

An overview of the integrated model architecture can be found in Figure 1. The route choice model (RCM) is coded in C++ and run in Microsoft Visual Studio 2022 with an academic license. The output for every RCM simulation consists of five .CVS files. The integrated infection and crowd behavior and model itself is coded in Python and run in Spyder. Every investigated case was repeated five times and the infection results in this paper correspond to an average over these five repetitions.

The parameters from Equation 2 are recognized in Figure 1 as start parameters, except the ventilation rate Q. This parameter is no longer a constant start parameter as the ventilation rate Q has become location specific based on the Air Change per Hour ACH, the location floor area and the space height H_c. The node occupancy and local ventilation rate is calculated using the start parameters and RCM output. The last step consists of the modified Wells-Riley infection risk calculation. The infection risk is given in a matrix format with the infection risk for every agent per timestep. The size of this matrix covers approximately 60000 time steps (rows) and 2848 agents (columns) for the total population. The exposure time is tracked for the time an agent stays in the same location and the exposure time is reset when an agent changes node location.

In the infection risk calculation, two assumptions have been made. The first assumption is related to the situation where the social distance is more than $10.8m$. At social distances greater than this, the social distance index becomes negative which results in a negative infection risk. This situation lies outside the scope of the modified Wells-Riley equation and one could question if there is infection risk at all when the infector and the susceptible agent are so far apart. Therefore, the infection risk is set to zero for negative social distance index results. The second assumption concerns the time when agents are not yet moving to their first destination or when agents have finished their activity schedule. The infection risks for these situations are also assumed to be zero. The assumption does not affect the risk calculations for the rest of the day as the exposure time is reset. The reasoning behind this assumption can be found in the fact that the implemented ship layout does not realistically model the guest and crew cabin spaces. For example, the guest cabins are modelled in large groups, as if agents are staying together in one large space. This situation leads to unexpected high risks before starting and after finishing the activity schedule. Also, the focus of this research is not the infection risk calculation for long-term risk inside a cabin, but infection risk during normal-day movement. Normal-day movement is still captured in the model results when the described assumptions are implemented.

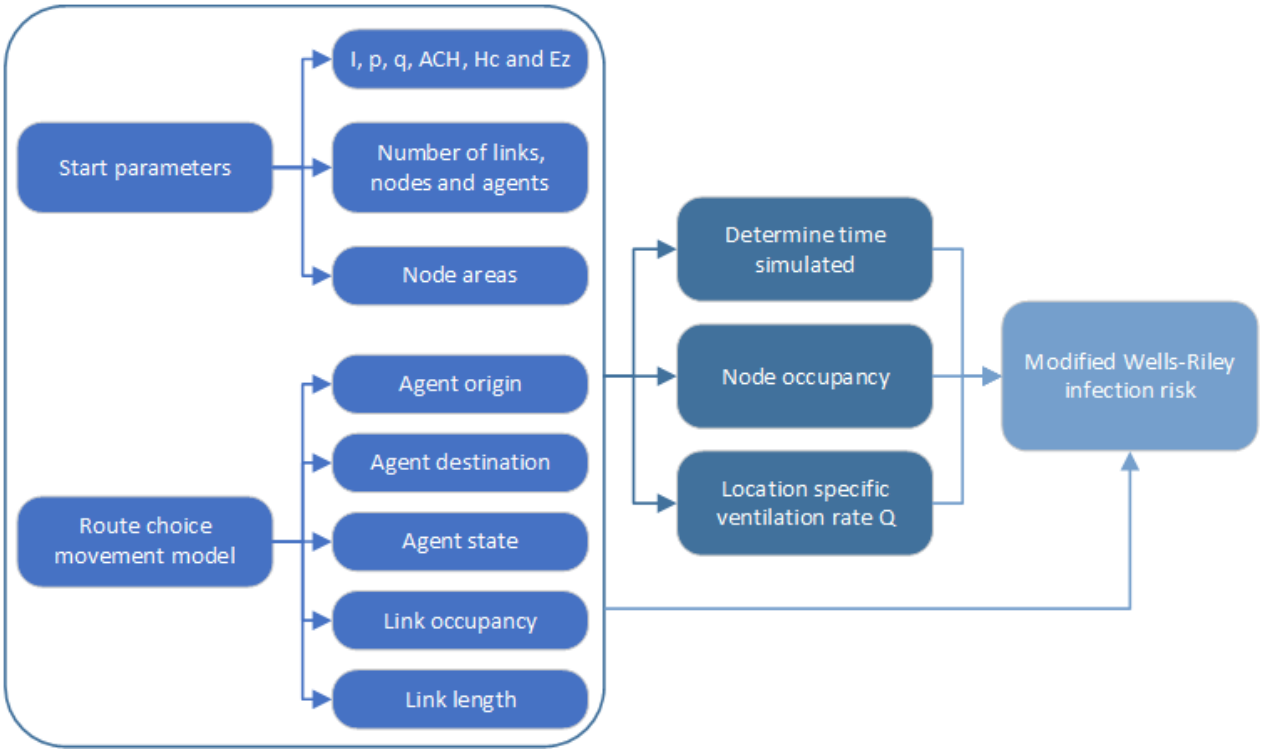

Figure 1: Integrated model architecture

SAMPLE CASES AND VALIDATION

This section presents two sample cases for the integrated infection and crowd behavior model. These sample cases are continuously presented as a reference when investigating ship layout adjustments, capacity reductions and mask wearing. The sample cases can be described covering three main topics: the ship layout, the activity schedule and the chosen start parameters. The ship layout is based on the second data-set from the SAFEGUARD project which features the layout from a cruise ship operated by Royal Caribbean International (Galea et al., 2012; Brown et al., 2021). The layout corresponds to the Radiance of the Seas cruise ship as seen in Figure 2. The ship characteristics are provided in Table 2. It is relevant to note that the Radiance of the Seas has undergone retrofitting after the SAFEGUARD project and the deck plans are no longer a complete match (Royal Caribbean Press Center, 2024). The current dataset is sufficient for this research as it does provide a realistic representation of 'a large passenger vessel'.

Figure 2: Radiance of the Seas (CruiseMapper, 2024)

Table 2: General characteristics Radiance of the Seas (Royal Caribbean Press Center, 2024)

Ship	Radiance of the Seas
Owner	Royal Caribbean Group
Maiden Voyage	7 April 2001
Tonnage	90,090 GT
Length (LOA)	293.2 m
Beam	32.2 m
Draft	8.63 m
Decks	13 (12 guest accessible)
Speed	25 kts

The activity schedule prescribes the node destinations per individual agent over the course of a day. The structure of the schedules can be found in Table 3 and Table 4. The guests complete seven legs per day: cabin → breakfast → activity → lunch → activity → dinner → activity → cabin. All agents follow the same trend (seven legs) but the activity and meal locations are chosen arbitrarily. The crew schedule specifies eight legs: cabin → shift → break → shift → break → shift → break → shift → cabin. The cruise ship can host over 850 crew of which 700 crew are modelled. These crew members have frequent contact with the guests.

Table 3: Sample case guest activity schedule characteristics

Number of agents	2148
Groups	Every 4 agents follow the same schedule
Activity/Meal duration	140 minutes $\pm$ 10 minutes
Moving to breakfast	Uniform distribution 08:00 till 09:00
Final move to cabin	Between 21:00 and 24:00

Table 4: Sample case crew activity schedule characteristics

Number of agents	700
Shift duration	180 minutes (4x)
Break duration	30 minutes (3x)
Early shift	07:30 $\pm$ 3 minutes till 21:00 $\pm$ 3 minutes
Late shift	10:30 $\pm$ 3 minutes till 00:00 $\pm$ 3 minutes

Next to the layout and schedule, the start parameters were investigated and defined. The start parameters can be found in Table 5. The I parameter is set to 1 infected person per space, introducing a fundamental assumption for the integrated model: the agent risk is determined 'as if there were a single infected agent in every space the agent enters'. In reality, there might be multiple infectors or no infectors at all in a particular space. However, tracking the actual amount of infectors would require the model to assign disease states like 'infected', 'susceptible' or 'recovered'. The model would then become a microscopic agent-based model while the choice has been made to work with a less complex risk-based model instead.

The pulmonary ventilation rate p is set to 8 L/min associated with resting, sitting and light indoor activities. The quanta production rate and air change per hour have a significant impact on the infection risk results. The quanta production rate q is set to 100qph as a compromise dealing with the variation for this medical parameter in literature (Gaddis and Manoranjan, 2021; Dai and Zhao, 2023; Buonanno et al., 2020). Increasing the ACH value to 25 or even 30 air changes per hour leads to lower infection risks in the integrated model. However, there is also research that suggests that higher ventilation rates might increase virus spread because droplets spread further (Ritos et al., 2023). This phenomenon is not captured in the integrated model as droplet spread itself is not modelled. This consideration, together with ventilation values mentioned in literature, led to the choice of 15 air changes per hour for the ACH parameter (Sodiq et al., 2021; Azimi et al., 2021; Zheng et al., 2016). The space height H_c is set to 2.35m and the ventilation index lies outside the scope of this research and is therefore determined to be 1.

Table 5: Start parameters for integrated model

I	1
p	8 L/min
q	100 qph
ACH	15
H_c	2.35 m
E_z	1
Number of links	968
Number of nodes	389
Number of agents	2848

The two sample cases were validated against similar cases presented in literature. Most COVID-19 studies onboard large passenger vessels present attack rates and reproduction numbers based on real-life cases (Rocklöv et al., 2021; Mizumoto and Chowell, 2020; Liu et al., 2020). These attack rates and reproduction numbers are retrospectively calculated. The National Institute for Infectious Diseases in Japan determined that over a 20-day COVID-19 outbreak, 22% of the population

onboard the Diamond Princess cruise vessel was “detected to have been infected with SARS-CoV-2” (Rosca et al., 2022). Using the average daily infection risk for sample case 1 (0.807%) and sample case 2 (1.05%), the attack rates were calculated to be 15% and 18% for a 20-day outbreak. This calculation directly removes infected cases from the susceptible population, assuming that infected cases isolate directly. Additionally, the average infection risk does not change over the 20-day period. In reality, infected individuals might not isolate because they are pre-symptomatic or asymptomatic and it is possible that symptomatic agents do no isolate at all. The result will be an increase of infected individuals in the agent population, increasing the average infection risk over time. The actual number of cases and therefore attack rate will thus be higher which explains the slight difference between the calculated attack rates for the sample cases and the value reported for the Diamond Princess outbreak.

The sample cases were also compared to the infection risk inside a single office space described by Dai and Zhao (2022) and a multi-room office space from the research by Srivastava et al. (2021). The single office space scenario in Dai and Zhao (2022) features the Wells-Riley infection risk equation adjusted to include a regression equation based on a CFD analysis. For a 40 m^2 office hosting six people, the infection risk over an eight hour period is described to be 13.2%. Using the developed integrated model, an infection risk of 19.6% was calculated. Differences might be attributed to the presence of portable air cleaners and the incorporation of complex air/particle circulation (CFD) in the research by Dai and Zhao (2022).

For the multi-office space, Srivastava et al. (2021) used a CFD tool to simulate the air-flow within a 59-person office geometry which resulted in an average infection risk of 3.10%. The average infection risk was calculated to be 1.97% implementing the integrated model while assuming the office space to be a single open space. Taking the geometry and calculation approach differences into account, equal results were not expected but the integrated model does present a result in the same range as the CFD-based average infection risk.

Specifically focusing on location based infection risks, the top 20 high-risk locations from sample case 1 were compared to 20 waiting rooms in an out-patient hospital building in Shenzhen, China (Li and Tang, 2021). The day average infection risk for the SC1 locations ranges between 0.75% and 3.58% with an average of 1.49%. The day average infection risks for the 20 hospital rooms ranges between 0.19% and 2.63% with an average of 0.79% (Li and Tang, 2021). Lastly, infection risk at one of the restaurants onboard was validated against a reception scenario with similar space characteristics, occupation and exposure time (Lelieveld et al., 2020). The average infection risk for the restaurant over a three hour exposure period was calculated to be 3.2% compared to 1.6% reported by Lelieveld et al. (2020).

SHIP LAYOUT DESIGN

The integrated model was used to investigate the effect of ship layout adjustments on COVID-19 infection risk. For sample case 1, the average infection risks per node and links are presented in Figure 3 and Figure 4. The average infection risk is calculated as the average risk over all agents at that location for a specific timestep. These values are then averaged over time. The figures show that the node locations reach average infection risks 10000 times higher than the infection risks at links. There is one outlier at node 107 with an average infection risk of 16.8% which is not completely visible in Figure 3 because of the limited y-axis. This outlier concerns a local schedule inconsistency which does not affect the full-scale infection risk results. The inconsistency was resolved for the combined tested measures. The modified Wells-Riley infection equation only covers airborne transmission and the occupancy and extended exposure times at nodes cause higher infection risks compared to the links.

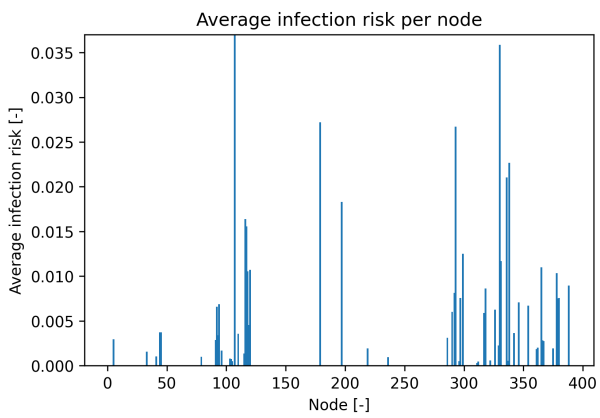

Figure 3: Average node infection risk (limited y-axis)

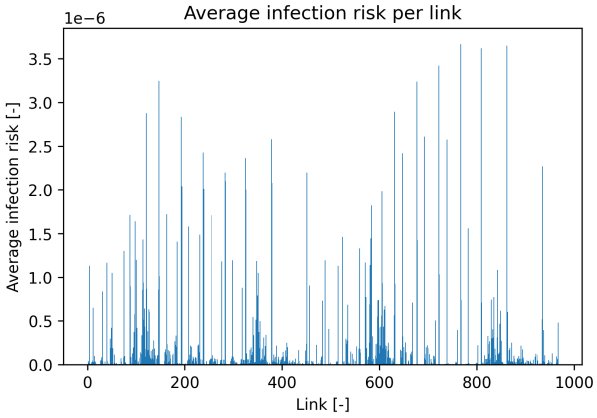

Figure 4: Average link infection risk

Based on the average infection risks and number of agents who reach their maximum infection risk at a certain node, two high-risk node locations were selected for further investigation. These nodes feature a restaurant on deck 11 (N293) and a restaurant on deck 12 (N330). The partial deck plans corresponding to these locations can be found in Figure 5 and Figure 6. The floor area of N293 was increased with $12m^2$, decreasing the area associated with neighboring corridor N295. The N330 restaurant is located next to a sundeck (N331) which was converted to become part of the N330 restaurant. The agents originally visiting the sundeck were relocated to adjacent sundeck nodes on the same deck.

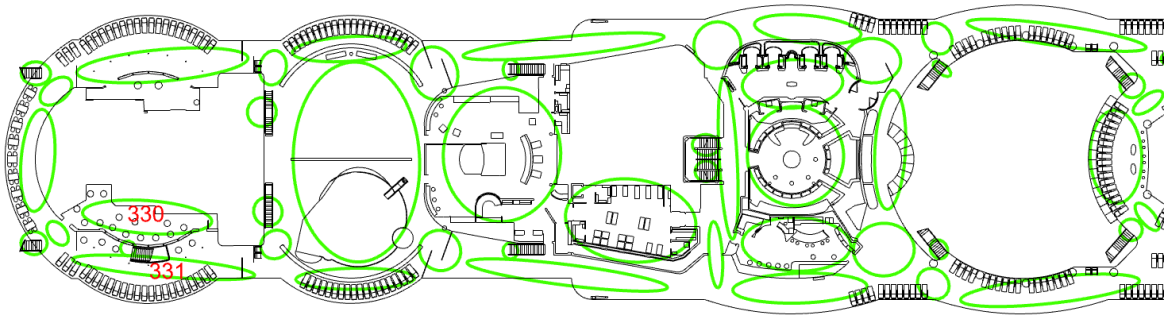

Figure 5: Deck 12 SAFEGUARD layout at N330 (Galea et al., 2012)

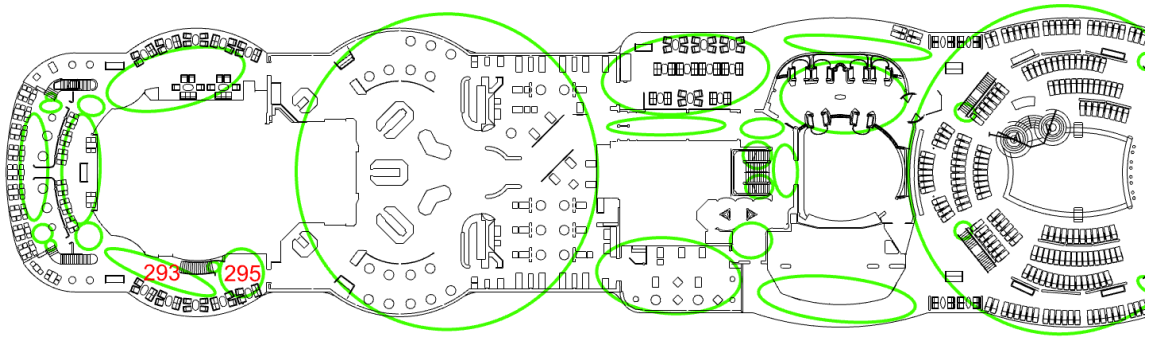

Figure 6: Deck 11 SAFEGUARD layout at N293 (Galea et al., 2012)

The location-specific infection risk for N293 and N330 can be found in Figure 7 and Figure 8. In Figure 7, there is a significant local risk improvement for the N293 restaurant. The average infection risk at N293 decreases to 1.57%, compared to 2.67% for sample case 1 (SC1) and 2.61% for sample case 2 (SC2). The N293 layout adjustment does not lead to higher infection risks for the surrounding nodes. Figure 8 presents a different picture as the N330 layout adjustment does not improve the local risk to a similar degree as the N293 adjustment. The average risk for N330 only decreases from 3.59% (SC1) or 3.51% (SC2) to 3.30% for the adjusted layout. The infection risk of adjacent node 331, which was converted from sundeck to restaurant, shows a risk increase to 1.57% compared to 1.17% for SC1 and 1.07% for SC2. The rerouted guests who are now using other sundecks do not significantly increase the infection risks for these sundeck nodes. If a local risk improvement for node 330 is to be achieved, a larger layout adjustment might be required. The N330 adjustment also shows that in trying to decrease the infection risk for a specific location, surrounding nodes might present with increased risk. This compromise should be considered whenever discussing layout adjustments in an effort to improve local infection risk.

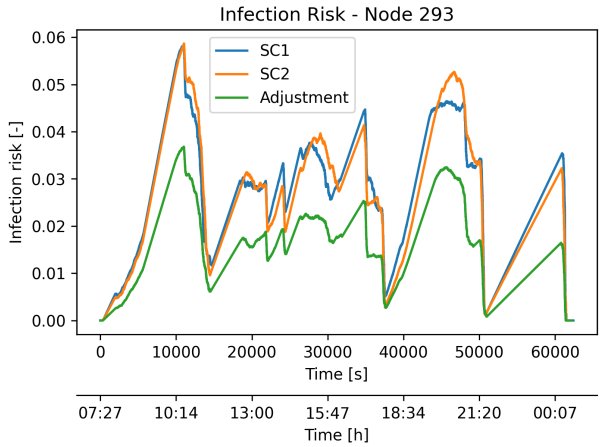

Figure 7: Infection risk at N293

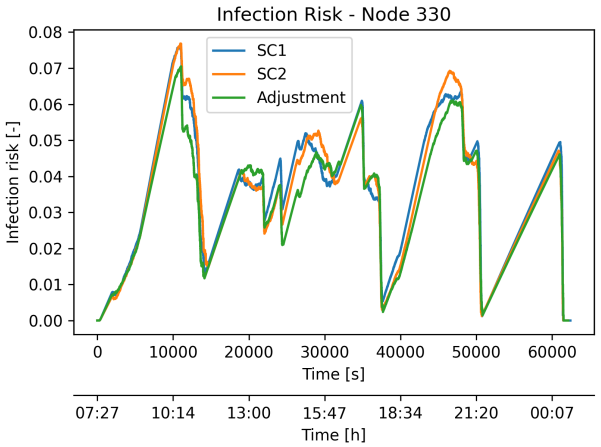

Figure 8: Infection risk at N330

Moving from local risk results to overall ship infection results, local improvements are not distinguishable from the risk variation related to the randomness in the route choice model output. This was expected as the layout adjustments were small compared to the size of the complete ship. Also, the agents affected by the layout change only cover part of the population. Thus, the improvements are simply too small to be visible in full-ship infection results even if local risk improvements are achieved.

CAPACITY REDUCTION

The integrated model was also used to test an operation measure, namely the capacity reduction for both the crew and guests. This measure was implemented for the following reductions CR = [2562, 2280, 1994, 1708, 1422, 1140, 711] agents corresponding to reduction percentages $CR = [10, 20, 30, 40, 50, 60, 75]\%$. The guest-to-crew ratio was kept constant and the reduced number of guests and crew was randomly removed from the activity schedule.

Figure 9 gives the total infection risk for the investigated capacity reductions. Sample case 1 and 2 are presented in the figure for 0.807% (SC1) and 1.05% (SC2). The average infection risk reveals a decreasing trend for increasing capacity reductions. The main mechanism behind this risk improvement can be related to increasing social distances through lower space occupancies. The average risk increase between 20% and 30% is unexpected but can be connected to the randomness in the integrated model input. This randomness is found in the population draws for the capacity reductions and in the route choice model outcomes used as integrated model input. This variation can also be recognized in the two sample cases for which the first sample case provides more favourable infection risk results. During the simulations, SC1 was used as a conservative reference in the sense that this sample already has low infection risks without any layout intervention or

implemented operational measures. Sample case 2 presents a more average situation related to infection risk. All capacity reductions lead to smaller infection risks than the second sample case with risk reductions from 4.8% (CR=10%) up to 40% (CR=75%). Compared to SC1, capacity reductions above 50% result 2.6% (CR=50%), 6.5% (CR=60%) and 22% (CR=75%) risk reductions.

In Figure 10, the percentage of the population with an infection risk above 50% over time is visualized. The capacity reduction below 50% are not presented in the figure as they only showed small improvements for the number of high-risk agents around 13:00. However, the capacity reductions above 50% show an infection risk improvement compared to sample case 2, especially for the risk peaks around 13:00 and 15:30. These times correspond to the end of the morning activity and the end of lunch.

Combining the results from Figure 9 and Figure 10, some general conclusions can be drawn. Improvements are achieved in the average infection risks, especially for higher capacity reductions. Additionally, for higher capacity reductions, the percentage of agents at high risk decreases compared to sample case 2. The improvements for smaller capacity reductions remain limited. A possible reason for this could be linked to the initial crowdedness onboard cruise vessels. When the number of guests and crew is slightly reduced, the ship remains crowded and social distance might not significantly improve. In this situation, large capacity reductions are required in order to achieve larger infection risk improvements. These increased capacity reductions might introduce issues around economic and operational feasibility. A possibility could be to implement a small capacity reduction as part of an intervention plan; also covering other operational or behavioral measures which together achieve infection risk improvements.

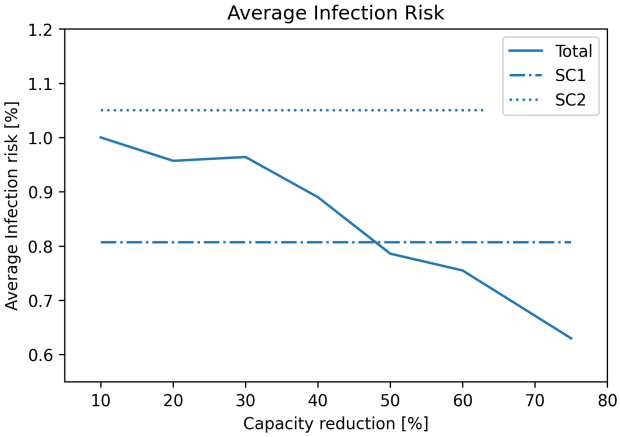

Figure 9: Average infection risk over CR

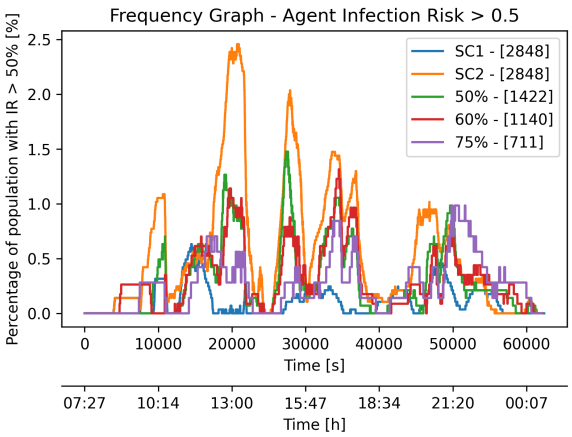

Figure 10: Infection risk above 50% for CR

MASK WEARING

A third investigated scenario is the behavioral intervention covering mask wearing by guests and crew. Mask wearing can be conveniently implemented in the modified Wells-Riley from Equation 2 through the definition of an adjusted pulmonary ventilation - and quanta production rate. The adjusted pulmonary ventilation rate is given in Equation 3 with respiratory filtration efficiency η_R. Equation 4 defines the adjusted quanta production rate q for an exhalation filtration efficiency η_E. The respiratory and exhalation filtration efficiencies are assumed to be 50% for surgical masks (Zheng et al., 2016; Dai and Zhao, 2020).

$$p_{adjusted} = p(1 - \eta_R) \tag{3}$$

$$q_{adjusted} = q(1 - \eta_E) \tag{4}$$

Three measure variations were formulated, specifying in which conditions guests and crew wear a mask. In the first case (MASK1), guests are wearing masks whenever they are moving between locations and crew members wear their masks continuously over the course of the day. The second case (MASK2) features a situation where guests are continuously wearing a mask except when they are at breakfast, lunch or dinner. The crew is, again, wearing their masks for the entire day. The final case (MASK3) relates mask wearing to the actual local social distance. In this situation, the crew and guests are obliged to wear a mask when the social distance becomes smaller than a specified safe distance. This safe distance is set to be $1.5m$ (CDC, 2020; European Centre for Disease Prevention and Control, 2023).

For all scenarios involving face masks, the average total risk results are lower than both sample cases as seen in Table 6. For MASK1, the average infection risk reduction is 2.4% compared to SC1 and 25% compared to SC2. This improvement can be solely attributed to a decreased risk for the crew who are wearing masks. The average guest risk shows no significant improvement compared to both SC1 and SC2. Notable average risk improvements are found for MASK2 and MASK3 with a risk reduction over 40% compared to SC1 and more than 50% compared to SC2. The guest infection risk for continuous and social distance-based mask wearing lie close together. A possible reason could be that the guests in MASK3 are almost continuously wearing a mask because the social distance is smaller than the set safe distance for the majority of the time.

Table 6: Average infection risks for mask wearing

Result [%]	SC1	SC2	MASK1	MASK2	MASK3
Average infection risk	0.807	1.05	0.787	0.451	0.487
Average guest infection risk	0.730	0.935	0.925	0.478	0.481
Average crew infection risk	1.04	1.39	0.362	0.369	0.506

Figure 11 presents the average infection risk over time for the three mask wearing scenarios. In scenarios MASK2 and MASK3, a pronounced risk decrease is recognized for the activities in between the meals around 13:00, 17:00 and after 21:30 for the evening activity. The 10:15 risk peak presents different behavior which can be explained by the fact that passengers do not wear a mask during breakfast. Continuing on this reasoning, the end of lunch peak around 15:30 and end of dinner peak around 20:00 are also expected to show less risk improvement. The figure indeed shows that for these timings there is little risk improvement for the tested cases compared to sample case 2.

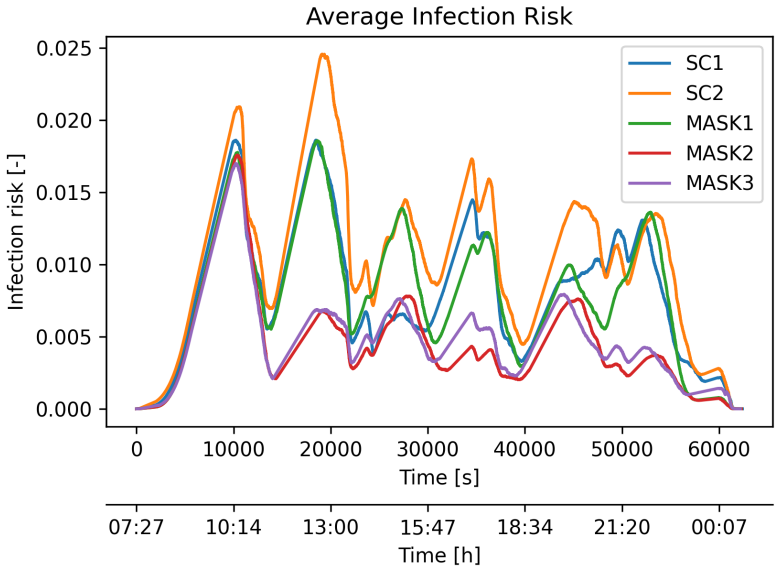

Figure 11: Average infection risk for mask wearing

In Figure 12, the guests at high risk are presented. MASK1 follows a similar trend as sample case 2, with a peak increase around 15:30. This increase might be the result of route choice model output variations. In general, wearing a mask solely during movement does not significantly improve the infection risks experienced by the guests. This matches with the findings for the ship layout design, where the nodes presented with higher infection risks than the links. The figure also shows that for MASK2 and MASK3, there are no guests with a risk above 50% except around 13:00. This is a major improvement compared to sample case 2. Looking at Figure 13, the crew at high risk is reduced for all scenarios involving masks, especially compared to SC2. The maximum number of crew members at high risk is 6 (MASK1-3) compared to 9 (SC1) and 38 (SC2) crew members.

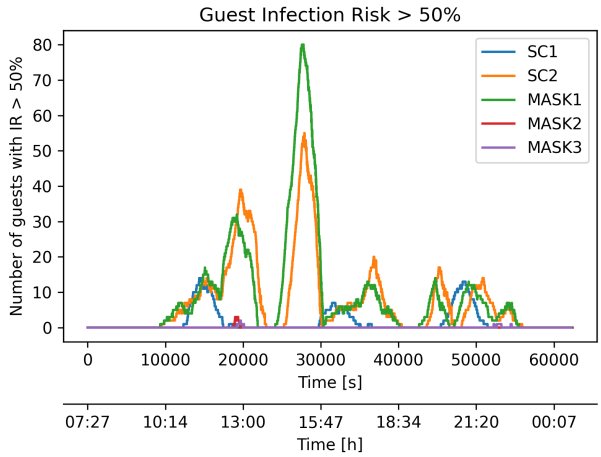

Figure 12: Guest infection risk above 50%

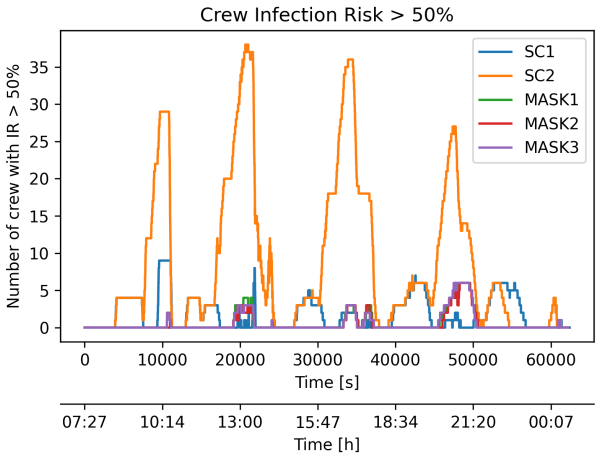

Figure 13: Crew infection risk above 50%

Continuous (MASK2) and social distance based mask wearing (MASK3) show most potential. Choosing between these two behavioral measures, with similar infection risk results, might instead be a question of preferred policy. Continuous mask wearing provides more clarity because guests and crew know when to wear a mask. Additionally, this measure avoids the situation where agents are frequently switching between mask on and mask off. Social distance based mask wearing could increase awareness around social distancing and crowded spaces. Guests might actually choose a different activity or route based on crowdedness and whether or not they have to wear a mask. Leaving these considerations aside, both measures do present significant average risk improvements and a reduction in the number of guests and crew at high risk.

COMBINED MEASURES

The previous sections described the implementation of capacity reduction, mask wearing and possible layout adjustments. The interventions can also be combined to further reduce COVID-19 infection risk. The combinations can be found in Table 7. The N293 layout adjustment was applied as it proved to decrease local infection risk without compromising surrounding nodes. The 50% capacity reduction is tested as this was the first scenario which presented with lower average risk results than sample case 1. Also, a 30% capacity reduction is investigated. This capacity reduction functions as a compromise between infection risk, profitability and operability. These two capacity reductions and N293 layout adjustment are combined with continuous mask wearing (MASK2) and social distance based mask wearing (MASK3).

Table 7: Specifications combined measures

	Layout adjustment	Capacity reduction	Mask wearing
C1	N293	CR = 30%	MASK2
C2	N293	CR = 50%	MASK2
C3	N293	CR = 30%	MASK3
C4	N293	CR = 50%	MASK3

The average infection risks are given in Table 8. The highest risk improvements are achieved for C1 and C2 when capacity reductions are combined with continuous mask wearing. The average risk from SC1 is reduced by 57% for C1 and by 64% for C2; compared to a 44% risk reduction when continuous mask wearing is applied as a stand-alone measure. The difference between a 30% and 50% capacity reduction is visible between C1 and C2 (-0.05%) and between C3 and C4 (-0.03%). Although, these differences seem rather small compared to the economic and operational impact that a 50% capacity reduction might have compared to a 30% capacity reduction. Figure 14 shows that for the combined cases, the average infection risk over time significantly decreases. The infection risk peak for breakfast does remain for the combined cases even as the other peak moments significantly decrease. A possible explanation for this is the fact that in a relatively short time, all guests move to breakfast and both crew shifts start in the same period. The movement of the guests still needs to spread out as they experience variations in activity duration over the day. For C1 and C3 there are no agents with an infection risk above 50%. C2 and C4 respectively have a maximum number of 2 guests and 2 crew with a risk above 50% at a single moment during the day. This is a significant improvement for the crew compared to Figure 13 for mask wearing without capacity reduction.

Table 8: Average infection risks for combined measures

Result [%]	SC1	SC2	C1	C2	C3	C4
Average infection risk	0.807	1.05	0.343	0.295	0.427	0.396

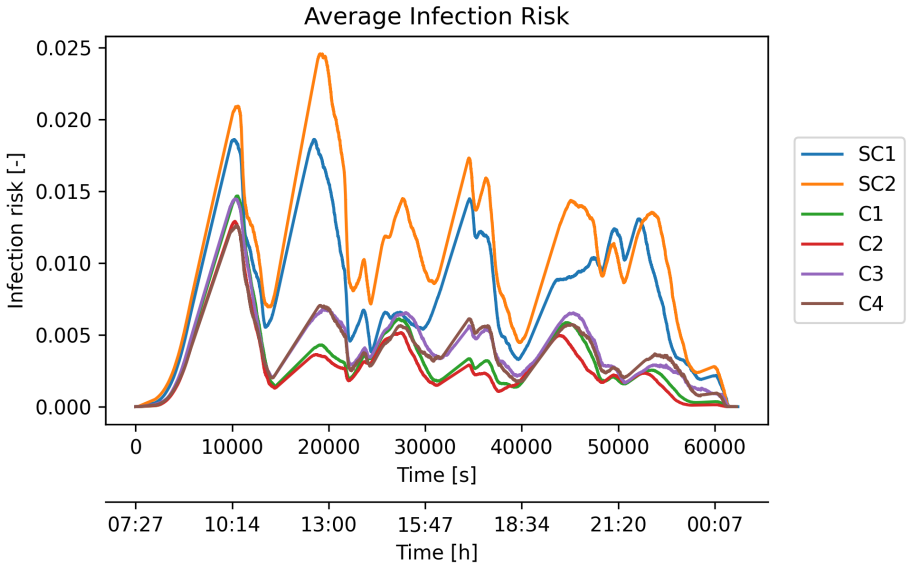

Figure 14: Average infection risk for C1-C4

DISCUSSION

The developed model presents a proof of concept for integrating a route choice movement model and a modified Wells-Riley infection model with the goal of investigating COVID-19 airborne infection risk onboard large passenger vessels. During the development and scenario evaluation, certain assumptions were required in order to move forward. These assumptions concerned the ship layout, agent activity schedule, compliance with implemented measures and chosen parameters. The infection results of the two sample cases revealed the variation related to the route choice model output. This in itself is also a strength of the integrated model because the movement of people is difficult to predict and should therefore feature a degree of randomness. However, to further improve the consistency of results it would be beneficial to increase the number of repetitions for further research. This also includes the repetition of population draws for the capacity reduction cases.

With respect to the integrated model, there are several areas available for further improvement and research. Firstly, the social distance calculation in the model is purely based on the location floor area and occupation. It was assumed that the agents distribute themselves over the available space and do not group together. In reality, the agents will probably group together and use the available space less efficiently, leading to smaller social distances and higher infection risks.

Secondly, the ship layout presents an opportunity for further improvement. The current layout does not model crew accommodation and the guest cabins are modeled in large groups. It could be interesting to implement a risk indication for the time agents spent in their cabins. This might require a different infection model than the one currently implemented. Also, the SAFEGUARD dataset was specifically created for the evaluation of large passenger evacuation models. During evacuations, elevators are not in use and they are thus not included in the current ship layout. These elevators are small spaces where agents stand close together, potentially resulting in high infection risks.

Thirdly, the integrated model only accounts for the airborne transmission of COVID-19. There are other modes of transmission, like contact transmission, which are relevant for infection risk onboard large passenger vessels because of the crowded spaces and shared (sanitary) facilities. These other transmission modes can increase the infection risks and specific control or preventive measures might show inferior or superior results when additional transmission modes are taken into account. Next to the transmission modes, there are medical parameters with a constant value that require further attention. For example, the pulmonary ventilation rate is constant for the integrated model. When someone is exercising in the gym, this ventilation rate will increase significantly and a crew member at work might have a higher pulmonary ventilation rate compared to the guests.

Suggestions for future research can move in either a microscopic or macroscopic direction. For the macroscopic direction, it is relevant to notice the boundaries of the current infection risk calculation, as the integrated model assumes the passenger vessel to be a confined environment without any outside influences. Additionally, the model is focused on infection risk and does not specify disease progression in terms of cases. If the ship were considered in its environmental setting, ports and travel routes become relevant because infected individuals might embark or disembark the vessel. In summary, the integrated model could be further developed describing cases over an extended period of time while incorporating the environmental setting of the passenger vessel.

Future research could also move in the microscopic direction, related to the ship layout, the investigated disease and the tested measures and adaptions. This research might describe an extended sensitivity study for the base cases where the activity schedule and the ship layout are radically changed. Additionally, the current research covered a COVID-19 application of the integrated model for a cruise vessel layout. The integrated model could also be applied to a large naval vessel or a ferry to investigate the risk of another contagious disease in different circumstances. A final suggestion beyond retrofit design is the option to determine infection risk performance for a set of initial stage design plans. This could provide infection risk insight before a ship design is finalized and the ship is built.

CONCLUSIONS

This paper aimed to: *Investigate the effect of ship layout design, capacity reduction and mask wearing on COVID-19 airborne infection risk onboard large passenger vessels*. This investigation is based upon the development of an integrated model that calculates agent-based infection risk, incorporating guest and crew circulation through a passenger ship layout. Various movement and infection models were studied in an effort to find the model combination that best fits the proposed model requirements. After careful consideration, a mesoscopic route choice model and a modified Wells-Riley infection model were selected for model integration. The integrated model was validated for two sample cases without any applied measures or layout adjustments.

Ship layout design, capacity reductions and mask wearing measures were evaluated using the integrated model. The node locations presented with higher infection risks than the links, caused by high occupancy and extended exposure time at nodes. The proposed layout adjustments resulted in local risk improvements. Investigating these layout changes is important as risk reduction for one location might lead to a risk increase somewhere else in the layout. For increasing capacity reductions, the average infection risk decreases. This is specifically visible for higher capacity reductions above 50%. A possible reason could be the initial busy and crowded environment onboard a large cruise ship, which requires large capacity reductions in order to achieve larger infection risk improvements. These large capacity reductions do raise questions regarding operational and economic feasibility. It might be interesting to combine a 'smaller' capacity reduction with other control or prevention measures like mask wearing. For the mask wearing scenarios, the highest average risk improvements from the three tested interventions were achieved. Continuous and social distance based mask wearing reduced the average risk over 40% compared to the sample cases.

When continuous mask wearing is combined with a 30% or 50% capacity reduction, average infection risk reductions over 55% are achieved compared to the sample cases. The average risk improvement between a 30% and 50% capacity reduction, combined with mask wearing, is relatively small compared to the economic and operational impact of a 50% capacity reduction. For all tested combined measures, there is a significant reduction in the number of agents that present infection risks above 50% over the course of a day.

Considering the evaluated infection risk for the different layout adjustments, measures and combined scenarios; the aim of this paper was reached using the developed integrated infection and crowd behavior model. Additionally, the model presents opportunities for further research and evaluation of different interventions, alternative ship layouts and application during the initial design stage.

CONTRIBUTION STATEMENT

N.A. de Haan Conceptualization; investigation; methodology; validation; visualization; writing – original draft. **A. A. Kana** Conceptualization; supervision; writing – review and editing **B. Atasoy** Conceptualization; supervision; writing – review and editing.

ACKNOWLEDGEMENTS

This work was performed as part of the academic thesis for the lead author, (de Haan, 2024). The thesis was performed in Marine Technology at Delft University of Technology and the authors would like to acknowledge Delft University of Technology for their support of this research.

REFERENCES

Azimi, P., Keshavarz, Z., Laurent, J. G. C., Stephens, B., and Allen, J. G. (2021). Mechanistic transmission modeling of COVID-19 on the Diamond Princess cruise ship demonstrates the importance of aerosol transmission. *PNAS*, 118.

Brewster, R. K., Sundermann, A., and Boles, C. (2020). Lessons learned for COVID-19 in the cruise ship industry. *Toxicology and Industrial Health*, 36(9):728–735.

Brown, R., Galea, E. R., Deere, S., and Filippidis, L. (2021). Passenger Response Time Data-sets for Large Passenger Ferries and Cruise Ships derived from sea trails. *International Journal of Maritime Engineering*, 155(A1).

Buonanno, G., Stabile, L., and Morawska, L. (2020). Estimation of airborne viral emission: Quanta emission rate of SARS-CoV-2 for infection risk assessment. *Environment international*, 141.

CDC (2020). Social distancing : keep a safe distance to slow the spread.

CruiseMapper (2024). Radiance Of The Seas deck plan.

Dai, H. and Zhao, B. (2020). Association of the infection probability of COVID-19 with ventilation rates in confined spaces. *Building Simulation*, 13(6):1321–1327.

Dai, H. and Zhao, B. (2022). Reducing airborne infection risk of COVID-19 by locating air cleaners at proper positions indoor: Analysis with a simple model. *Building and Environment*, 213:108864.

Dai, H. and Zhao, B. (2023). Association between the infection probability of COVID-19 and ventilation rates: An update for SARS-CoV-2 variants. *Building Simulation*, 16(1):3–12.

European Centre for Disease Prevention and Control (2023). Questions and answers on COVID-19: Travelling.

Gaddis, M. D. and Manoranjan, V. S. (2021). Modeling the Spread of COVID-19 in Enclosed Spaces. *Mathematical and Computational Applications*, 26(79).

Galea, E., Deere, S., and Filippidis, L. (2012). THE SAFEGUARD VALIDATION DATA SET – SGVDS2 A GUIDE TO THE DATA AND VALDIATION PROCEDURES. Technical report, University of Greenwich.

Guagliardo, S. A. J., Prasad, P. V., Rodriguez, A., Fukunaga, R., Novak, R. T., Ahart, L., Reynolds, J., Griffin, I., Wiegand, R., Quilter, L. A., Morrison, S., Jenkins, K., Wall, H. K., Treffiletti, A., White, S. B., Regan, J., Tardivel, K., Freeland, A., Brown, C., Wolford, H., Johansson, M. A., Cetron, M. S., Slayton, R. B., and Friedman, C. R. (2022). Cruise Ship Travel in the Era of Coronavirus Disease 2019 (COVID-19): A Summary of Outbreaks and a Model of Public Health Interventions. *Clinical Infectious Diseases*, 74(3):490–497.

Gupta, A., Kunte, R., Goyal, N., Ray, S., and Singh, K. (2021). A comparative analysis of control measures on-board ship against COVID-19 and similar novel viral respiratory disease outbreak: Quarantine ship or disembark suspects? *Medical Journal Armed Forces India*, 77:S430–S436.

Healthy Sailing (2024). Prevention, mitigation, management of infectious diseases on cruise ships and passenger ferries.

Kak, V. (2007). Infections in Confined Spaces: Cruise Ships, Military Barracks, and College Dormitories.

Kasper, M. R., Geibe, J. R., Sears, C. L., Riegodedios, A. J., Luse, T., Von Thun, A. M., McGinnis, M. B., Olson, N., Houskamp, D., Fenequito, R., Burgess, T. H., Armstrong, A. W., DeLong, G., Hawkins, R. J., and Gillingham, B. L. (2020). An Outbreak of Covid-19 on an Aircraft Carrier. *New England Journal of Medicine*, 383(25):2417–2426.

Keçeci, T. (2022). Importance and applicability analysis of the health and safety measures taken against the coronavirus disease on merchant vessels Tuba KEÇECİ. *Aquatic Research*, 5(3):171–185.

Kordsmeyer, A. C., Mojtahedzadeh, N., Heidrich, J., Militzer, K., Münster, T. v., Belz, L., Jensen, H. J., Bakir, S., Henning, E., Heuser, J., Klein, A., Sproessel, N., Ekkernkamp, A., Ehlers, L., de Boer, J., Kleine-Kampmann, S., Dirksen-Fischer, M., Plenge-Bönig, A., Harth, V., and Oldenburg, M. (2021). Systematic review on outbreaks of sars-cov-2 on cruise, navy and cargo ships. *International Journal of Environmental Research and Public Health*, 18(10):5195.

Lelieveld, J., Helleis, F., Borrmann, S., Cheng, Y., Drewnick, F., Haug, G., Klimach, T., Sciare, J., Su, H., and Pöschl, U. (2020). Model Calculations of Aerosol Transmission and Infection Risk of COVID-19 in Indoor Environments. *International Journal of Environmental Research and Public Health*, 17(8114).

Li, C. and Tang, H. (2021). Study on ventilation rates and assessment of infection risks of COVID-19 in an outpatient building. *Journal of Building Engineering*, 42:103090.

Li, H., Meng, S., and Tong, H. (2021). How to control cruise ship disease risk? Inspiration from the research literature. *Marine Policy*, 132:104652.

Lipsitch, M., Chan, H. T., Emery, J. C., Russell, T. W., Liu, Y., Hellewell, J., Pearson, C. A., Covid, C., Group, W., Knight, G. M., Eggo, R. M., Kucharski, A. J., Funk, S., Flasche, S., and MGJ Houben, R. (2020). The contribution of asymptomatic SARS-CoV-2 infections to transmission on the Diamond Princess cruise ship. *eLife*.

Liu, F., Li, X., and Zhu, G. (2020). Using the contact network model and Metropolis-Hastings sampling to reconstruct the COVID-19 spread on the "Diamond Princess". *Science Bulletin*, 65(15):1297–1305.

Mangili, A. and Gendreau, M. A. (2005). Transmission of infectious deceases during commercial air travel. *Lancet*, 365:989–996.

Mizumoto, K. and Chowell, G. (2020). Transmission potential of the novel coronavirus (COVID-19) onboard the diamond Princess Cruises Ship, 2020. *Infectious Disease Modelling*, 5:264–270.

Moon, J. and Ryu, B. H. (2021). Transmission risks of respiratory infectious diseases in various confined spaces: A meta-analysis for future pandemics. *Environmental Research*, 202.

Mouchtouri, V. A., Nichols, G., Rachiotis, G., Kremastinou, J., Arvanitoyannis, I. S., Riemer, T., Jaremin, B., and Hadjichristodoulou, C. (2010). State of the art: public health and passenger ships. *International maritime health*, 61(2):53–98.

Narayan, J., Kana, A., Atasoy, B., and Alonso-Mora, J. (2021). Activity and Agent Based Simulation Model with Path-Size Logit Mixture for Passenger Flow to Evaluate Ship Layout. Unpublished.

Nicolaides, C., Avraam, D., Cueto-Felgueroso, L., González, M. C., and Juanes, R. (2020). Hand-Hygiene Mitigation Strategies Against Global Disease Spreading through the Air Transportation Network. *Risk Analysis*, 40(4):723–740.

Noakes, C. J., Beggs, C. B., Sleigh, P. A., and Kerr, K. G. (2006). Modelling the transmission of airborne infections in enclosed spaces. *Epidemiology and Infection*, 134(5):1082–1091.

Ritos, K., Drikakis, D., and Kokkinakis, I. W. (2023). Virus spreading in cruiser cabin. *Physics of Fluids*, 35(10).

Rocklöv, J., Sjödin, H., and Wilder-Smith, A. (2021). COVID-19 outbreak on the diamond princess cruise ship: Estimating the epidemic potential and effectiveness of public health countermeasures. *Journal of Travel Medicine*, 27(3):1–7.

Rosca, E. C., Heneghan, C., Spencer, E. A., Brassey, J., Plüddemann, A., Onakpoya, I. J., Evans, D., Conly, J. M., and Jefferson, T. (2022). Transmission of SARS-CoV-2 Associated with Cruise Ship Travel: A Systematic Review. *Tropical Medicine and Infectious Disease*, 7(10).

Royal Caribbean Press Center (2024). Radiance of the Seas Fact Sheet.

Ruggiero, V., Guglielmino, E., and Filippo, C. (2008). An interactive approach for the design of an Italian fast medical support ship as consequence of world emergency due to Sars2-Covid 19. *International Journal on Interactive Design and Manufacturing*, 16:409–417.

Sodiq, A., Khan, M. A., Naas, M., and Amhamed, A. (2021). Addressing COVID-19 contagion through the HVAC systems by reviewing indoor airborne nature of infectious microbes: Will an innovative air recirculation concept provide a practical solution?

Srivastava, S., Zhao, X., Manay, A., and Chen, Q. (2021). Effective ventilation and air disinfection system for reducing coronavirus disease 2019 (COVID-19) infection risk in office buildings. *Sustainable Cities and Society*, 75.

Sun, C. and Zhai, Z. (2020). The efficacy of social distance and ventilation effectiveness in preventing COVID-19 transmission. *Sustainable Cities and Society*, 62:102390.

Tan, S., Zhang, Z., Maki, K., Fidkowski, K. J., and Capecelatro, J. (2022). Beyond well-mixed: A simple probabilistic model of airborne disease transmission in indoor spaces. *Indoor Air*, 32(3).

Turvold, W. and Mcmullin, J. (2020). Ships Become Dangerous Places During a Pandemic. *Asia-Pacific Center for Security Studies*.

van Gisbergen, D. (2022). Development of a crowd behavioral model for large-scale simulation on large vessels. Technical report, Delft University of Technology, Delft.

Yazir, D., Şahin, B., Yip, T. L., and Tseng, P. H. (2020). Effects of COVID-19 on maritime industry: a review. *International Maritime Health*, 71(4):253–264.

Zhao, X., Liu, S., Yin, Y., Zhang, T., and Chen, Q. (2022). Airborne transmission of COVID-19 virus in enclosed spaces: An overview of research methods. *Indoor Air*, 32(6):e13056.

Zheng, L., Chen, Q., Xu, J., and Wu, F. (2016). Evaluation of intervention measures for respiratory disease transmission on cruise ships. *Indoor and Built Environment*, 25(8):1267–1278.